A. W. Vinal

A Magnetic Sensor Utilizing an Avalanching Semiconductor Device

A new semiconductor device for sensing uniaxial magnetic fields has been realized. The device is basically a dual-collector open-base lateral bipolar transistor operating in the avalanche region, and is referred to as a Magnetic Avalanche Transistor. It exhibits high magnetic transduction sensitivity compared to traditional Hall-effect and conventional nonlinear magnetoresistive devices. Several hundred experimental devices have been designed, fabricated, and tested over the past two years. Many structural and some process parameters were varied. The magnetic sensitivity of a typical device was found to be proportional to substrate resistivity. A sensitivity of 30 volts per tesla was measured for devices which used 5-ohm-cm p-type substrates. The output signal measured between collectors is differential and responds linearly with field magnitude and polarity. A typical signal-to-noise ratio is 20 000 per tesla. The bandwidth is known to extend well beyond 5 MHz. The sensitive area is calculated to be on the order of 5 μ m². This communication describes the basic structure, fabrication, and characteristics for the magnetic avalanche transistor.

Introduction

This communication reports on a new solid state magnetic-sensing device referred to as the Magnetic Avalanche Transistor (MAT). Basically this device is a dual-collector open-base lateral bipolar transistor which operates in the avalanche region. The magnetic field sensitivity of the device is high compared to the Hall-effect and magnetoresistive sensors. The sensitivity of the device to a magnetic field is strongly related to its static *I-V* characteristics.

Many applications require sensing broad-band magnetic fields. In its present form, the MAT is a candidate for sensing fields in excess of 0.5 mT. Other solid state magnetic sensors based on Hall or conventional nonlinear magnetoresistive effects have been built, but these possess limitations in comparison to magnetic avalanche transistors, as illustrated by the data of Table 1. For example, the Hall effect, even applied to semiconductors, is limited in sensitivity to about 0.1 volt per tesla.

The Magistor [4], invented by E. C. Hudson, Jr., is a dual-collector *planar* transistor operating below ava-

lanche breakdown with beta values in the range of 30 to 100. In effect, this beta appears to amplify a typical Hall voltage. The sensitive axes are orthogonal to the substrate surface. This device is not included in Table 1. Sensitivities $S_{\rm T}$ and $S_{\rm R}$, for example, can be obtained for this device by multiplying the Hall cell entry by an average beta value of 50.

Magnetoresistive elements may exhibit an order of magnitude better sensitivity than Hall cells but are generally characterized by nonlinear, and in some cases undirectional and biaxial, transduction mechanisms.

Magnetic sensors usually require broad bandwidth and linear, high-gain amplifiers to transform small signals to useful amplitudes. The available signal cannot be amplified exclusively of random noise or other undesirable signals introduced by thermal or mechanical stress effects. The gain-bandwidth requirements of such amplifiers are as high as 10¹⁰ in order to reproduce signals with 10⁷-Hz characteristics.

Copyright 1981 by International Business Machines Corporation. Copying is permitted without payment of royalty provided that (1) each reproduction is done without alteration and (2) the *Journal* reference and IBM copyright notice are included on the first page. The title and abstract may be used without further permission in computer-based and other information-service systems. Permission to *republish* other excerpts should be obtained from the Editor.

Table 1 Comparison of solid state magnetic sensors.

Device	$Transduction \\ sensitivity \\ S_{\rm T} \\ ({\rm volts~per~tesla})$	Intrinsic signal-to- noise (per tesla)	Number of sensitive axes	Resistive sensitivity S_R (volts per ampere-tesla)	range	Output signal		Dimensions of sensitive area				Amplifier gain-bandwidth
						Bi- polar	Differ- ential		Υ (μm)	Z (nm)	Α (μm²)	requirements (Hz)
MAT	30	20,000	1	3750 at 4 mA per collector	0.2 T	Yes	Yes	5	1	20	5	2×10^7
Thin film MR	2 (a)	5000 (b)	2	110 at 15 mA	$5 \times 10^{-3} \mathrm{T}$	No	No	50	16	30	800	1 × 10 ⁹
Hall cell	0.1	3000	1	50 at 2 mA	1.0 T	Yes	Yes	25	25	$\frac{2\times}{10^3}$	625	1×10^{10}
SOS mag- neto- diode	3.6 (+B) (d) 0.9 (-B) at 100 mA diode current	1,000,000 at 10 kHz (e)	_	40 (+B) 10 (-B) at 100 mA diode current	_	Yes (c)	No	-	10	2 × 10 ⁴	-	3 × 10 ⁸ at 100 mA diode current

Abbreviations, table headings, and notes

- MR—Magnetoresistive; SOS—Silicon-on-sapphire; T—tesla [note: | gauss = 10⁻⁴ tesla].
- Intrinsic signal-to-noise ratio—Ratio of signal-to-internal noise per tesla. Data specified for bandwidth of 1 MHz.
- Number of sensitive axes—Uniaxial sensitivity is preferable
- Resistive sensitivity: S_R—Output signal per ampere per tesla.
- Linear range—Maximum field (in tesla units) that can be sensed before nonlinear transduction occurs.
- Output signal:

In the following sections the device geometry, the fabrication, and experimental tests and data obtained for a number of MAT devices investigated are presented. The experimental section includes information on static *I-V* characteristics, magnetic response, sensitivity and collector-current dependence, noise characteristics, frequency response, life test, and application circuits.

Device geometry

Figures 1 and 2 are top and cross-sectional views, respectively, of a magnetic avalanche transistor. Seven fundamental structural elements are illustrated. Two collector diffusion regions are shown spaced apart from one another within the substrate. The separation distance or "slit width" between the collector regions is typically 2.5 μ m. An emitter is located between the collectors and emitter contact. The depth of the emitter, approximately 2.5 μ m, is similar to the depth of the emitter contact diffusion.

A relatively shallow $(1-\mu m)$ control resistance $R_{\rm E}$ couples the emitter to the emitter contact. The length of this region is greater than two diffusion lengths for excess minority carriers and is typically 60 μm long and 16 μm wide. This region is implanted and then diffused to obtain precise control of the resistance.

- Bidirectional—Output signal polarity coincides with field polarity.
- Differential—Both output terminals operate at essentially the same potential.
- Dimensions of sensitive area—Small dimensions lead to high-resolution sensing.
 Amplifier gain-bandwidth product—Criteria based on 10-MHz bandwidth. 10⁻¹
- tesla field, and 1-volt output.

 (a) 5 × 10⁻³ T or greater flux density produces 8-mV maximum signal response. See Refs. [1, 2].
- (b) 350-μV noise level produced by Barkhausen effects. See Refs. [1, 2].
- (c) Nonlinear transduction with field direction.
- (d) +B and -B refer to the direction of the magnetic field. See Ref. [3].
- (e) Signal-to-noise was specified at 10 kHz only. See Ref. [3].

A metal shield or accelerator is shown to overlap a portion of the collector, the emitter, and the control resistance; this shield forms an integral part of the emitter contact. The metal shield is insulated from the semiconductor surface by an oxide layer approximately 600 nm thick, except for the oxide layer over the ionization promoter region which is typically 100 nm thick.

The base is measured from the end of the emitter to the end of the space-charge region extending from the collectors. The length of the base region is approximately equal to the excess majority carrier diffusion length. No electrical connection is made to the base. The resulting configuration is a three-terminal, linear differential magnetic field sensor.

Fabrication

The starting wafers for experimental devices are p-type silicon with (100) orientation. After cleaning, a 200-nm oxide layer to be used for masking is grown in steam. Standard photoresist and etching techniques and three separate diffusions are used to achieve the desired geometry and doping of the various regions of the device.

The emitter contact, emitter, and collectors exclusive of their tips are formed in the first diffusion of phos-

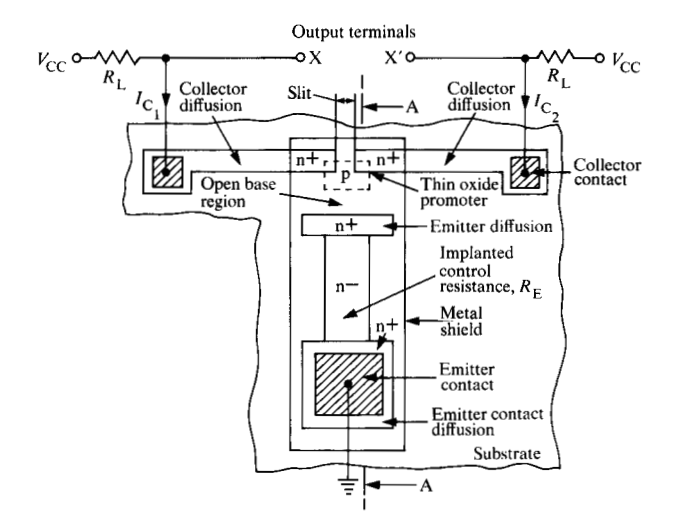


Figure 1 Basic dual-collector structure.

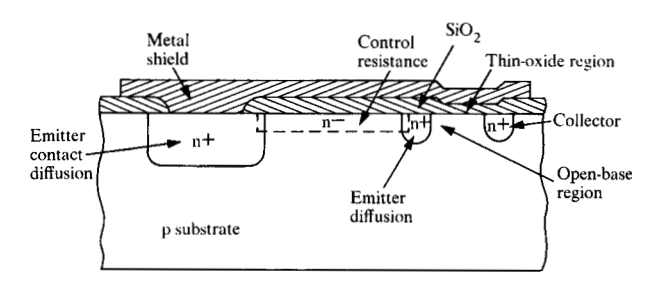


Figure 2 Cross section A-A.

phorus. Subsequently, a combined drive-in/oxidation is carried out in steam, resulting in an oxide of 700 and 800 nm grown over the substrate and diffusion regions, respectively. The resistivity of this diffusion is 10 ohms per square. Essentially, the same masking and etching techniques are used to define the second and third diffusion regions. The second diffusion process develops the emitter control resistance region. For this diffusion, phosphorus is implanted and drive-in is accomplished simultaneously with a reoxidation step. The third diffusion defines the relatively shallow tips of the collectors and is accomplished in a similar manner.

The desired separation between the collector regions is obtained through mask design by allowing for lateral growth of the collector regions during drive-in. The final separation distance between the collectors is approximately 2.5 μ m.

After the final diffusion is formed, a clean thermal oxide is grown over the ionization promoter region. Finally,

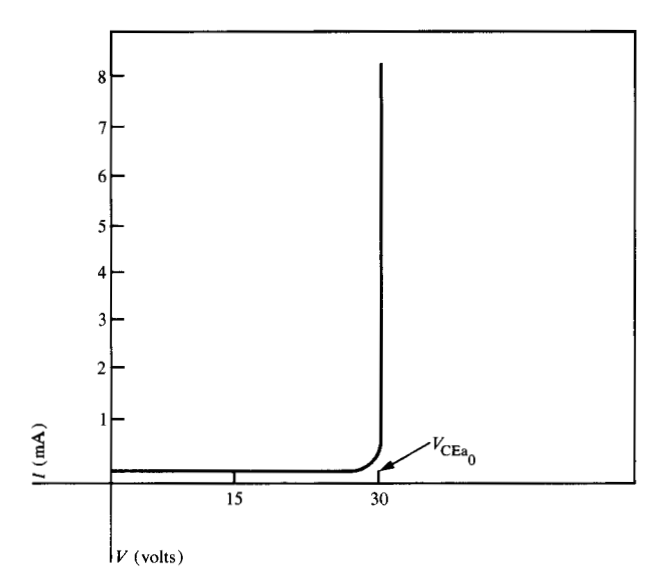


Figure 3 Device characteristics: static voltage-current property.

contacts are opened, metal is evaporated, and interconnections are formed.

Tests and data

• Static I-V characteristics

Several hundred experimental dual-collector magnetic sensors have been examined. Most of the devices had the basic structural characteristics illustrated by Fig. 1. Variational differences resulted from the effects of the length-to-width ratio and doping of the emitter control resistance, the space between the collector regions, the length of the transport region, collector diffusion depth and resistivity, and promoter oxide thickness.

All identical devices fabricated within the test series exhibited very repeatable static and dynamic properties. A picture of the preferred vertical static V-I characteristics desired for the device (see Fig. 3) was obtained from a curve tracer by connecting both collectors together and by grounding the emitter contact. Many devices in the test series exhibited a predominately positive or negative slope pivoting about the avalanche threshold voltage $V_{\rm CEa.}$. The variations experienced were the result of investigating the effects that base length, base resistivity, and emitter control resistance had on adjusting transport efficiency alpha. The resistivity and aspect ratio of the emitter control resistance, Fig. 1, may be adjusted during device manufacture. This structural feature provides a versatile means to control emitter injection efficiency and thereby achieve the desired vertical V-I avalanche property. The critical value of the emitter control resistance depends on avalanche area, substrate (base) resistivity, and the length of the transport region. Figure 4 shows the dependence on base resistivity.

• Magnetic response

The transistor configuration shown in Fig. 1 has been operated as a magnetic sensor in both avalanche and nonavalanche modes. In both modes, the orientation of the magnetic field is normal to the substrate surface. It has been observed that the magnetic response signal polarity for the nonavalanche mode is 180° out of phase with the avalanche mode signal. It is believed that the dominant magnetic transduction mechanism exists within the emitter depletion region when the device is operated below avalanche potential, and within the ionization region of the collectors when it is operated above avalanche breakdown. The nonavalanche mode requires external application of a base current; the magnetic response signal increases in proportion to that current. The relative sensitivity of a device operated in the nonavalanche mode is approximately 1/20 of that measured for the same device operated at the same collector current in the avalanche mode. However, emitter current was at least one order of magnitude greater than for the same device operated in the avalanche mode. The same load resistors were used in the comparative test. The high-frequency response characteristics of the avalanche-mode device were found to be quite superior, with improvement in the signal-to-noise ratio. It is believed that these differences result from the much lower driving-source impedance of the dual-collector device when it is operated in the avalanche mode. Driving-source impedance is experimentally determined by use of an external resistor connected between collectors. The shunt resistance is adjusted in value until 50% of the output signal amplitude is obtained. The shunt resistor is then measured and is equal in value to the driving source impedance of the sensor (500 ohms is typical for devices operated in the avalanche mode).

An applied magnetic field of 0.04 sin $(120\pi t)$ tesla was used to induce the device response shown. The time-varying output of the device is measured as a differential voltage between the collectors. A sensitivity of 30 V/T is typical for 5- Ω -cm p-type material. The linear range of the transduction mechanism permits an output voltage swing, at each collector, of approximately \pm 6 V.

• Sensitivity and its collector current dependence

Each device examined in the avalanche mode exhibited a typical increase in magnetic signal response with collector current. Output signal ceases to increase when total collector current is dominated by carrier multiplication within the avalanche area of the collectors. This saturation effect is illustrated in Fig. 5, where differential mag-

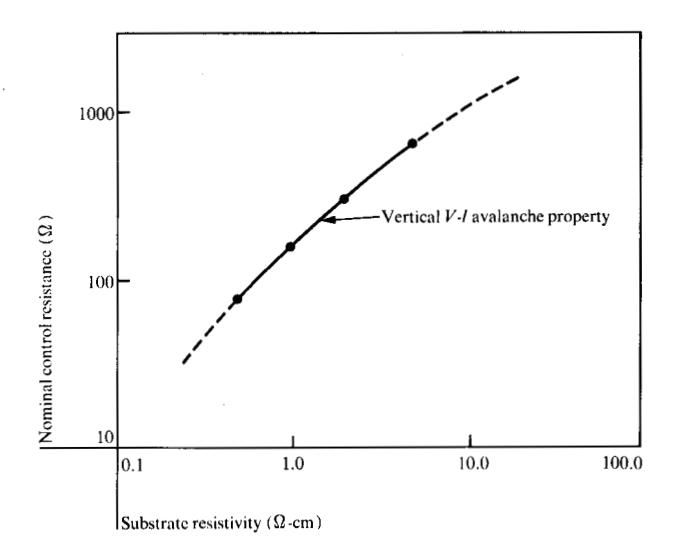


Figure 4 Control resistance as a function of substrate resistivity.

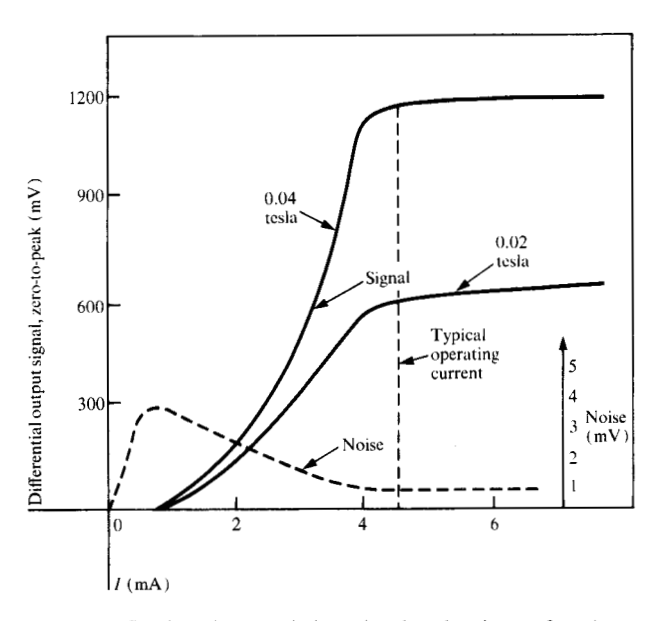


Figure 5 Device characteristics: signal and noise as functions of collector current.

netic signal amplitude and noise are plotted vs. collector current. Test conditions for this data are as follows:

- 1. 5- Ω -cm p-type silicon substrates with $\langle 100 \rangle$ orientation.
- 2. $2.5-\mu m$ slit width.
- 3. $0.04 \sin (120\pi t)$ -tesla field.

This current saturation property is not to be confused with linear magnetic signal behavior. Magnetic signal linearity prevails despite the fact that devices may be operated in the current saturation region.

199

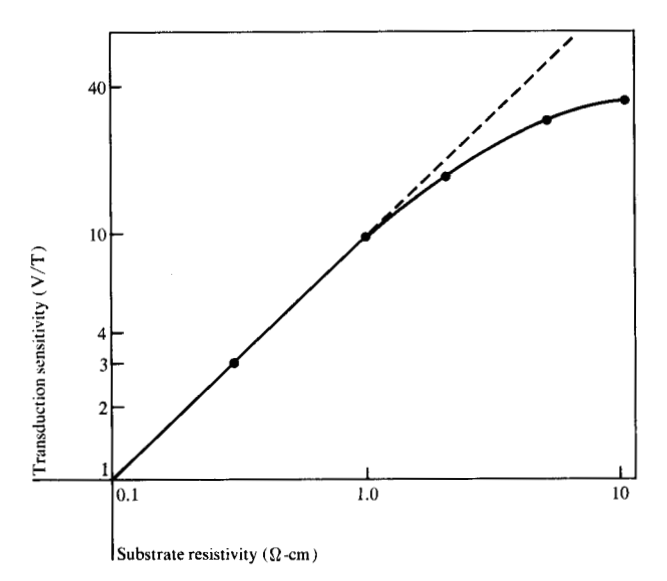


Figure 6 Sensitivity as a function of substrate resistivity. Base width = 2×10^{-3} cm; slit width = $2.5 \,\mu$ m.

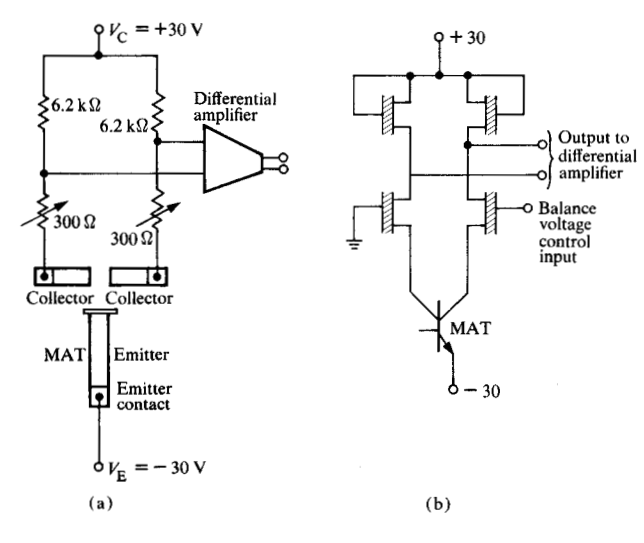


Figure 7 Method of dc-coupling to a differential amplifier: (a) discrete component circuit; (b) silicon-on-sapphire equivalent integrated circuit.

Figure 6 is a plot of transduction sensitivity measured from devices fabricated on wafers of different resistivity. It is clear from the data that sensitivity varies inversely with acceptor concentration. It is of particular interest to note the manner in which the maximum differential magnetic signal in volts per tesla varies with substrate resistivity. For example, 2- Ω -cm and 0.1- Ω -cm substrate resistivities lead to devices exhibiting a magnetic sensitivity of approximately 20 V/T and 1.0 V/T, respectively. This linear relationship appears to break down for substrate resistivities in excess of 5 Ω -cm.

Noise characteristics

There are two fundamental types of noise which interfere with magnetic field sensing. Intrinsic noise has its origin within the sensing device. Extrinsic noise may be electrical but also results from unwanted magnetic field components which are sensed along an axis perpendicular to the primary field sensing axis. Sensors with an orthogonal axis sensitivity ratio of 1 to 50 or less are usually acceptable and are considered to be uniaxial.

The average intrinsic signal-to-noise ratio S/N measured for typical magnetic avalanche transistor test devices was 20 000 per tesla, given a substrate resistivity of $5~\Omega$ -cm. A bandwidth of 1 MHz is used in the measurements for the purpose of standardization. This intrinsic S/N ratio is characteristic of devices which use thin oxide layers as the ionization promoter. The spectrum of the intrinsic noise was measured and an inverse frequency characteristic was observed extending from 0 Hz to 35 MHz. The high-frequency components are limited by stray capacitance within the test fixture.

The noise amplitude varied considerably for devices fabricated with different collector-diffusion techniques and different emitter-control-resistance geometry. In all cases, however, the intrinsic noise was at a minimum with devices having vertical V-I characteristics. Most of the 1/f noise is believed to be created by generation and recombination mechanisms occurring within the collector ionization region, and possibly enhanced by surface states within the Si-SiO, interface zone of the thin oxide promoter of the collectors. This conclusion was reached after comparing noise characteristics of devices operating above and below avalanche potential. The same collector current was established in both tests. Noise in the nonavalanche mode was typically one order of magnitude less and the spectra shifted away from the dominant 1/fcharacteristics observed for the avalanche mode. Temperature dependence of noise is currently unknown.

Noise was found to be considerably below average in devices which used $3-\mu$ m-deep collector diffusions exhibiting approximately 10 ohms per square. Such devices exhibited a S/N ratio of approximately 60 000 per tesla given the same 1-MHz bandwidth. The intrinsic noise factor given herein corresponds to the average condition observed between the low and high values measured.

• Frequency response

The response of typical devices to 3-mT pulsed magnetic fields has been measured. A 30-turn coil wound on a 0.65-cm-diameter ferrite core was energized by a 500-mA current pulse with a 200-ns rise time. All devices that were utilized in the frequency response measurements repro-

duced the current pulse characteristics, suggesting that the device has frequency capabilities considerably in excess of the 5 MHz demonstrable by the simple test. It is believed that the upper limit of frequency response is determined by depletion layer, stray capacity, and transit-time effects. Preliminary calculations suggest that a potential of 10⁹ Hz capability may exist.

• Life test

Several devices which used a thin oxide region as the ionization promoter and which exhibited the nominal vertical V-I property have been operating continuously for more than 25 000 hours at room temperature. The transduction sensitivity, breakdown voltage, and noise remain constant after an initial burn-in time of approximately 18 hours during which the noise spectrum shifted upwards in frequency, the breakdown voltage increased by about 10%, and the transduction sensitivity remained constant.

• Application circuit

Figures 7(a) and 7(b) illustrate one method of dc-coupling the magnetic avalanche transistor to a dc differential amplifier. In this configuration, two potential sources are used. The negative emitter potential $V_{\rm E}$ is used to set the dc level of the MAT collectors. If $V_{\rm E}$ is adjusted to correspond to $V_{\rm CEa_0}$ (initial avalanche breakdown voltage), the dc collector potential will be at ground level independently of quiescent avalanche collector current. The positive collector potential $V_{\rm C}$ is used to bias the sensor into the avalanche region. This potential may be gated off if it is desired to suppress sensing magnetic fields during some desired interval. The load resistors for each collector consist of a fixed resistor connected in series with low-resis-

tance MOS resistors. One or both MOS resistor gates can be used to manually or automatically balance the dc differential voltage coupling the sensor to the amplifier. An offset potential of about 200 mV is typical of MAT devices. A differential driving-source impedance of 500 Ω is also typical at nominal operating conditions.

Acknowledgments

The author wishes to acknowledge the following people for their support and encouragement: R. L. Cuttino, Semiconductor Technology, Dept. D62, IBM Corporation, Raleigh, North Carolina; and L. K. Monteith, Dean of Engineering, North Carolina State University.

References

- R. D. Hempstead, "Thermally Induced Pulses in Magnetoresistive Heads," IBM J. Res. Develop. 18, 547-550 (1974).
- C. H. Bajorek, C. Coker, L. T. Romankiw, and D. A. Thompson, "Hand-held Magnetoresistive Transducer," *IBM J. Res. Develop.* 18, 541-546 (1974).
- G. Kamarinos, P. Vicktorovitch, S. Cristoloveanu, J. Borel, and R. Staderini, "Characterization of Thin Silicon Films Based on Their Magnetosensitiveness," Proceedings of the Seventh International Vacuum Congress and the Third International Conference on Solid Surfaces, Vienna, 1977, p. 1943.
- 4. Robert H. Cushman, Ed., "Transistor Responds to Magnetic Fields," *Electronic Design News*, Feb. 15, 1969, pp. 73-78.

Received June 30, 1980; revised December 16, 1980

The author is located at the IBM System Communications Division laboratory, Research Triangle Park, North Carolina 27709.